Electronic Supporting Information

A new pyridoxal based fluorescence chemo-sensor for detection of Zn(II) and its application in bio imaging

Senjuti Mandal,[a] Yeasin Sikdar,[a] Dilip K. Maiti,[a] Guru Prasad Maiti,[b] Sushil Kumar Mandal,[c] Jayanta Kumar Biswas,[c] Sanchita Goswami[a*]

[a] Department of Chemistry, University of Calcutta, 92, A. P. C. Road, Kolkata – 700009, India. E-mail: sgchem@caluniv.ac.in

[b] Department of Molecular Biology and Biotechnology, University of Kalyani, Kalyani-741235, West Bengal, India.

[c] Department of Ecological Engineering & Environmental Management, University of Kalyani, Kalyani, Nadia-741235, West Bengal, India.

Contents **Page No.**

Chart 1 : Examples of tautomerism encountered in literature.

Serial No.	Ligands used	Sensed species	Type of tautomerism	Reference
1	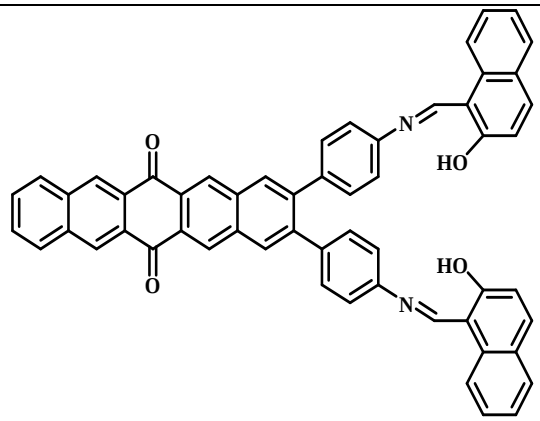	Zn^{2+}	Keto-enol	13(a)
2	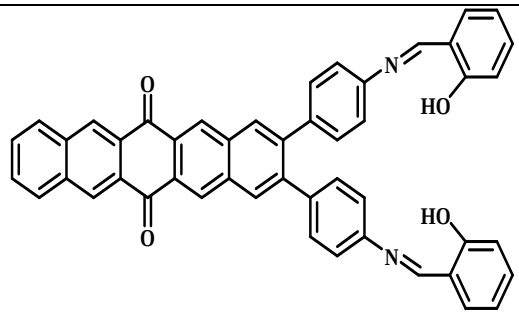	Zn^{2+}	Keto-enol	13(b)
3	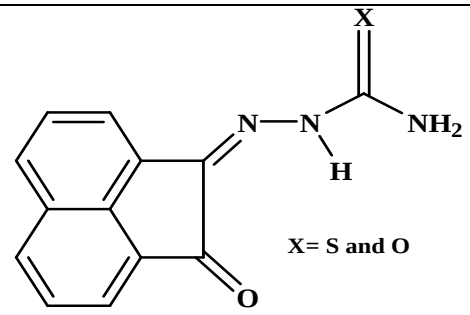	F^-	Azo-hydrazone	13(c)

4	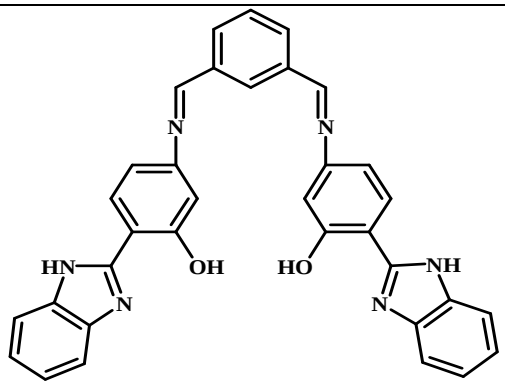	Zn^{2+}	Keto-enol	13(d)
5	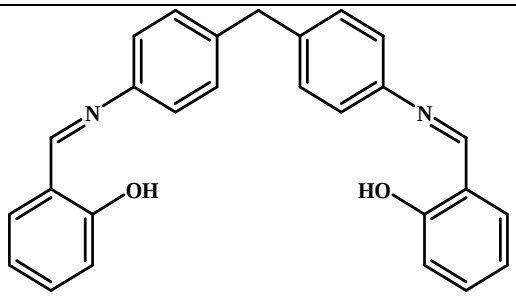	Al^{3+},ClO_4^-	Keto-enol	13(e)
6	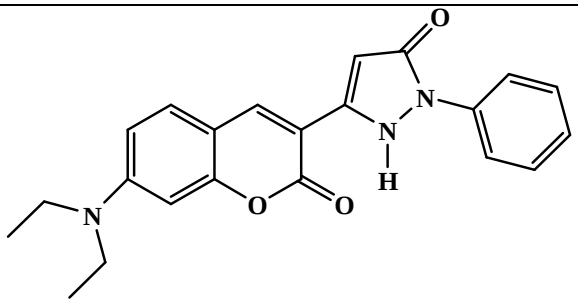	F^-	Keto-enol	13(f)
7	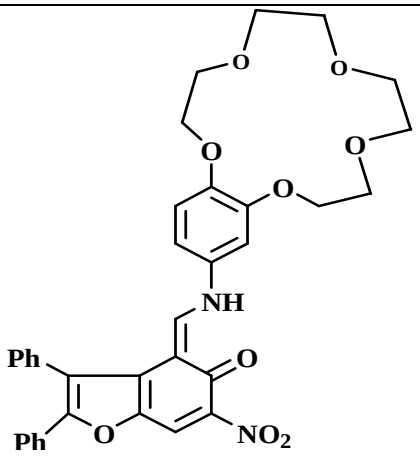	Mg^{2+},Ca^{2+}	Benzenoid-quinoid tautomerism	13(g)

	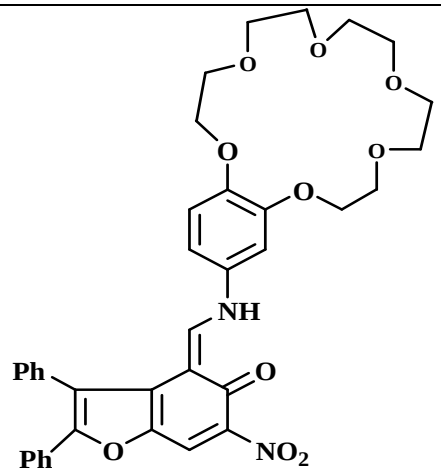	Ba^{2+}		
8	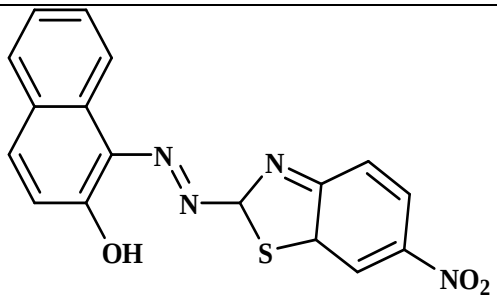	Hg^{2+}	Azo-hydrazone	13(h)
9	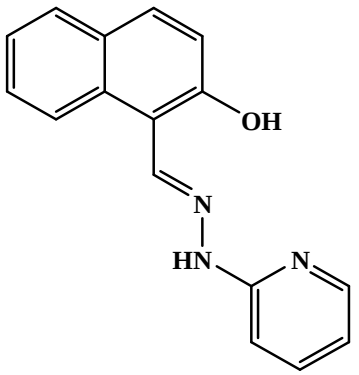	F^{-}	Azo-hydrazone	13(i)

	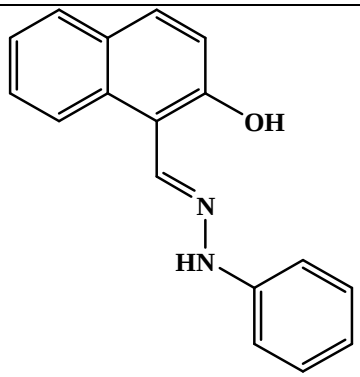 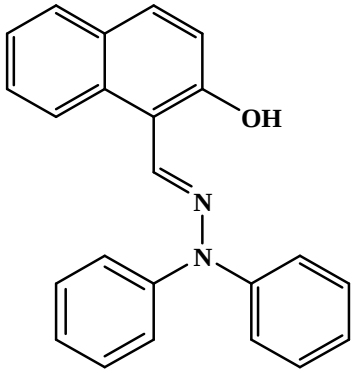 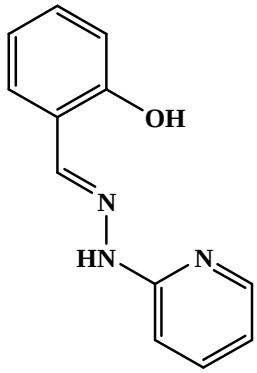			
10	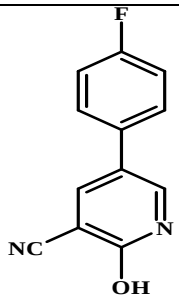	F^-, AcO^-, $H_2PO_4^-$	Keto-enol	13(j)

11	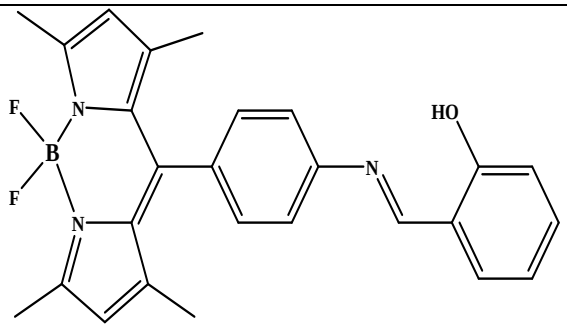	Cu^{2+}	Enol-imine keto-enamine	13(k)
12	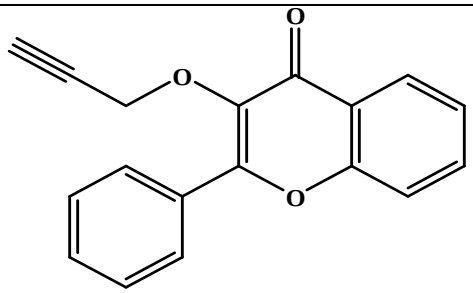	Pd^{2+}	Keto-enol	13(l)

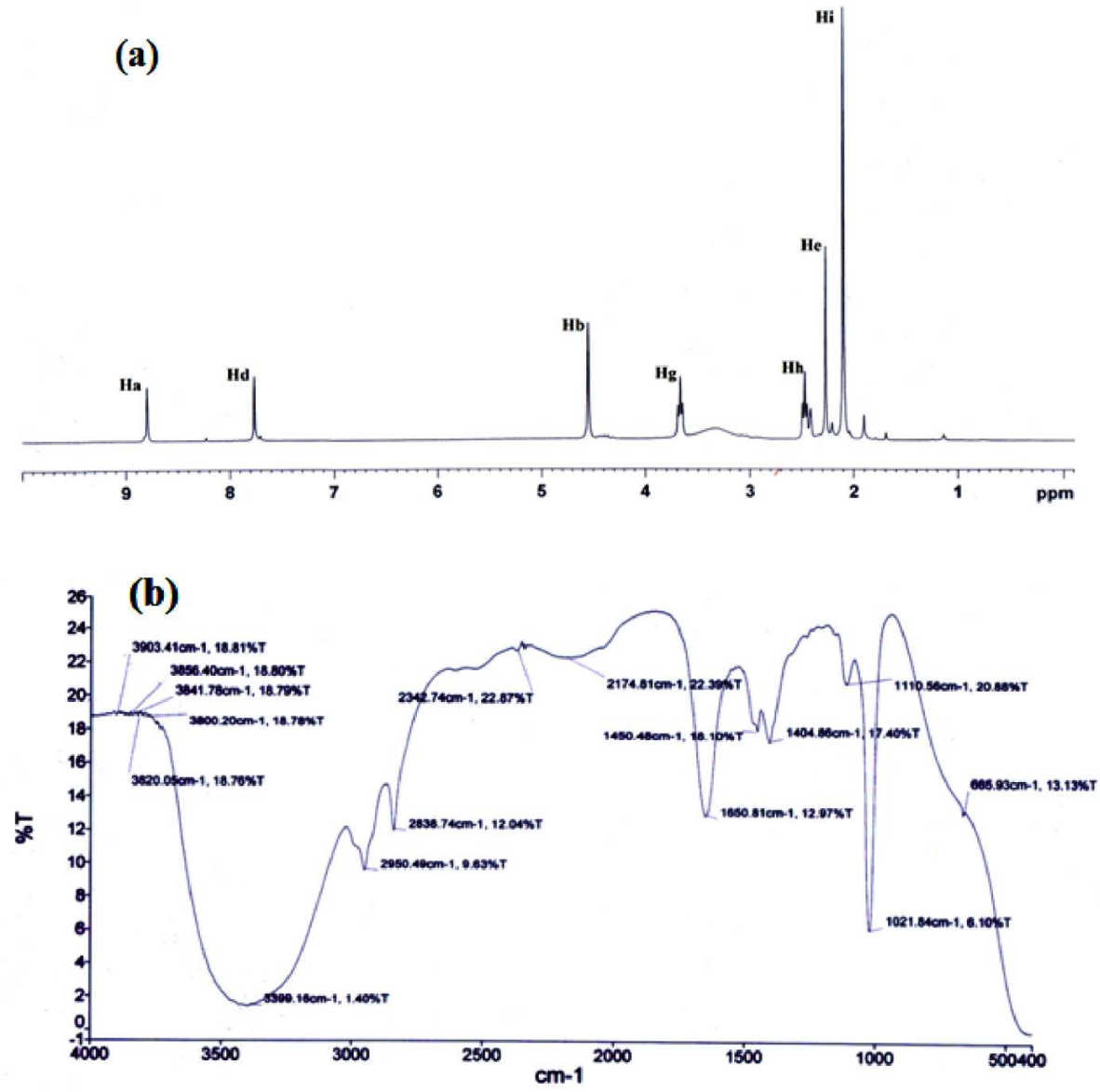

Figure S1: (a) ^{1}H NMR spectra of **PydDmen** in DMSO-d_6, (b) FTIR spectra of **PydDmen.**

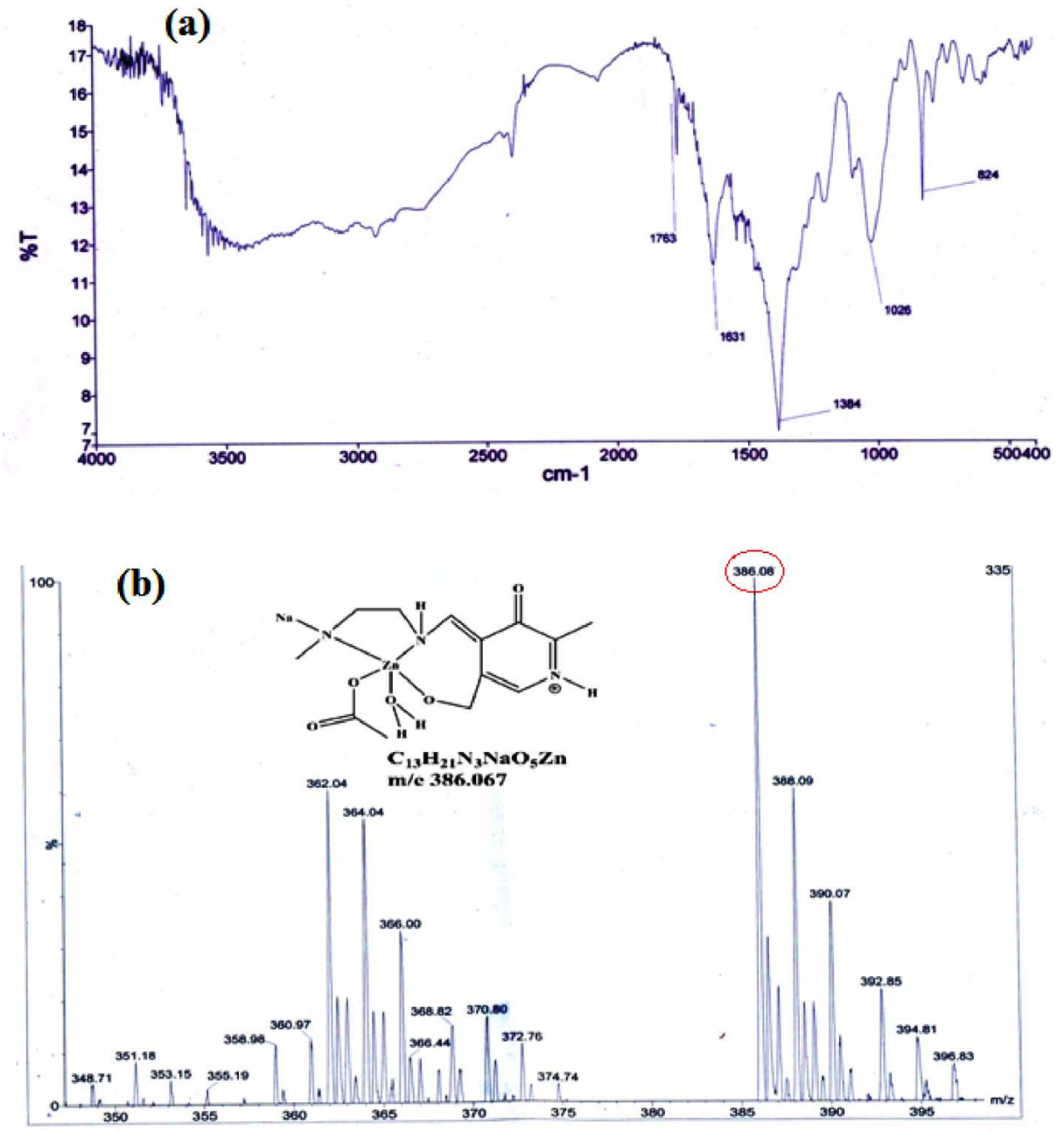

Figure S2: (a) FTIR spectra of **PydDmen-Zn^{2+}**, (b)ESI-MS of **PydDmen-Zn^{2+}** in methanol.

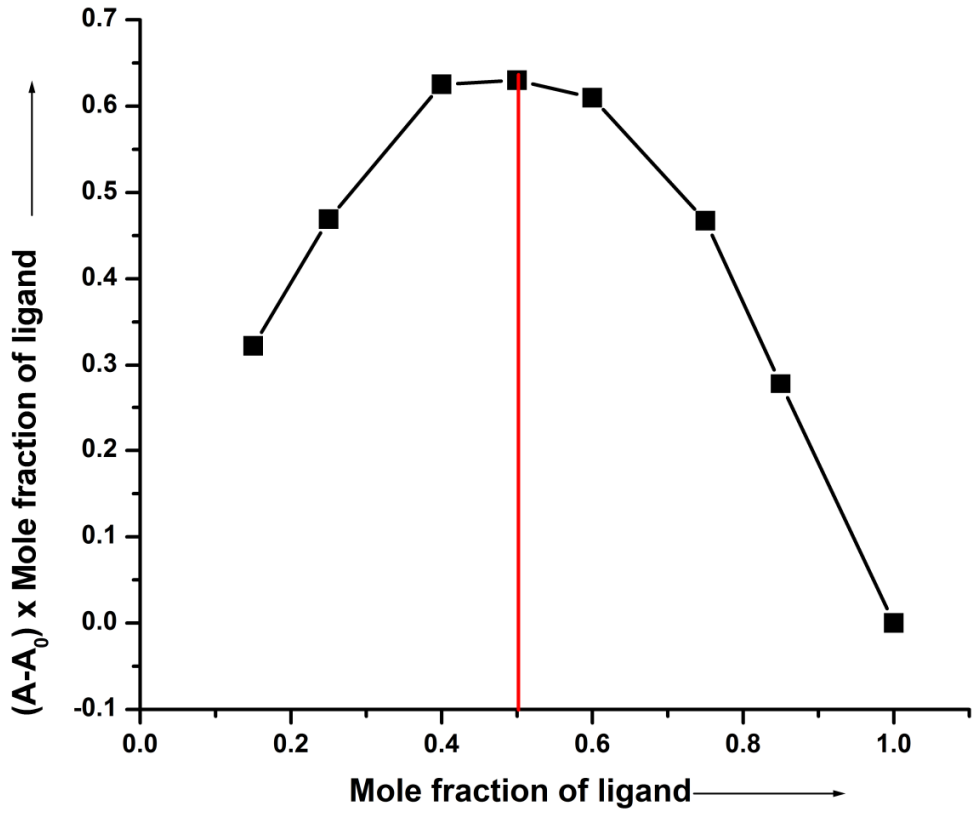

Figure S3: Job′s plot for the determination of **PydDmen-Zn^{2+}** (1:1) complex stoichiometry.

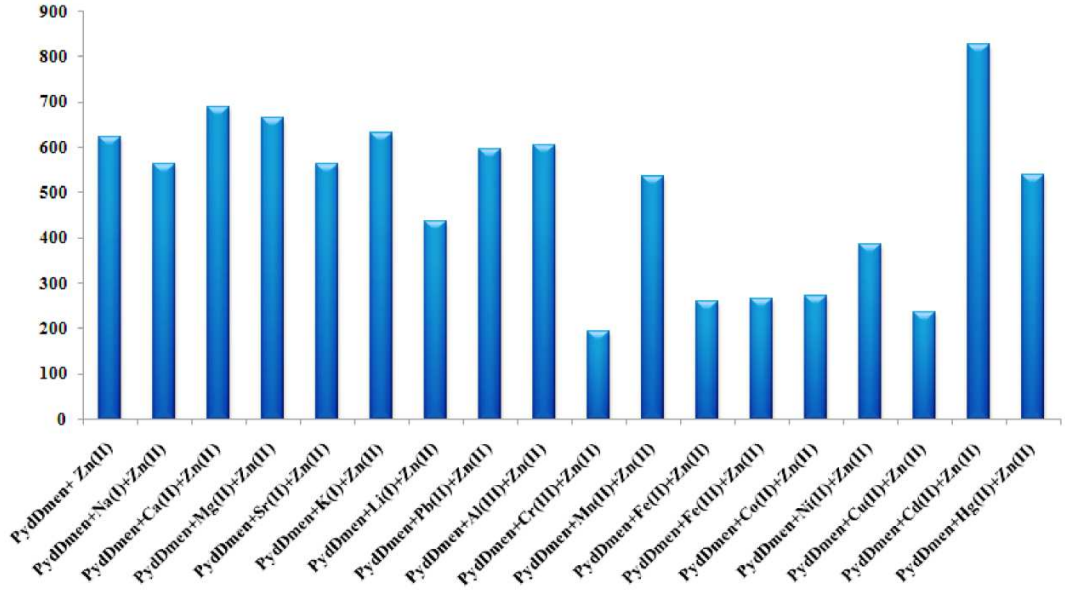

Figure S4: Relative emission intensity change profile of the chemosensor **PydDmen** ($5X10^{-6}$ M) in presence of 14 equiv. of various metal ions at 25°C in EtOH/ H_2O (4:1, v/v) in tris buffer at pH 7.4 (λ_{ex} =411 nm).

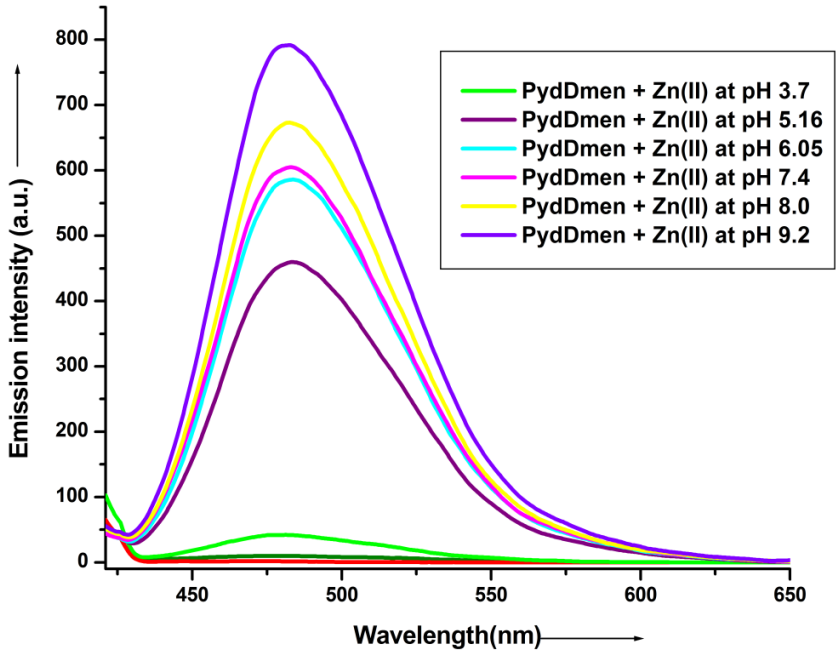

Figure S5: Effect of the pH on the fluorescence intensity of **PydDmen** ($5x10^{-6}$ M) in the presence of 14 equiv. of Zn^{2+} ions (λ_{ex}=411 nm).

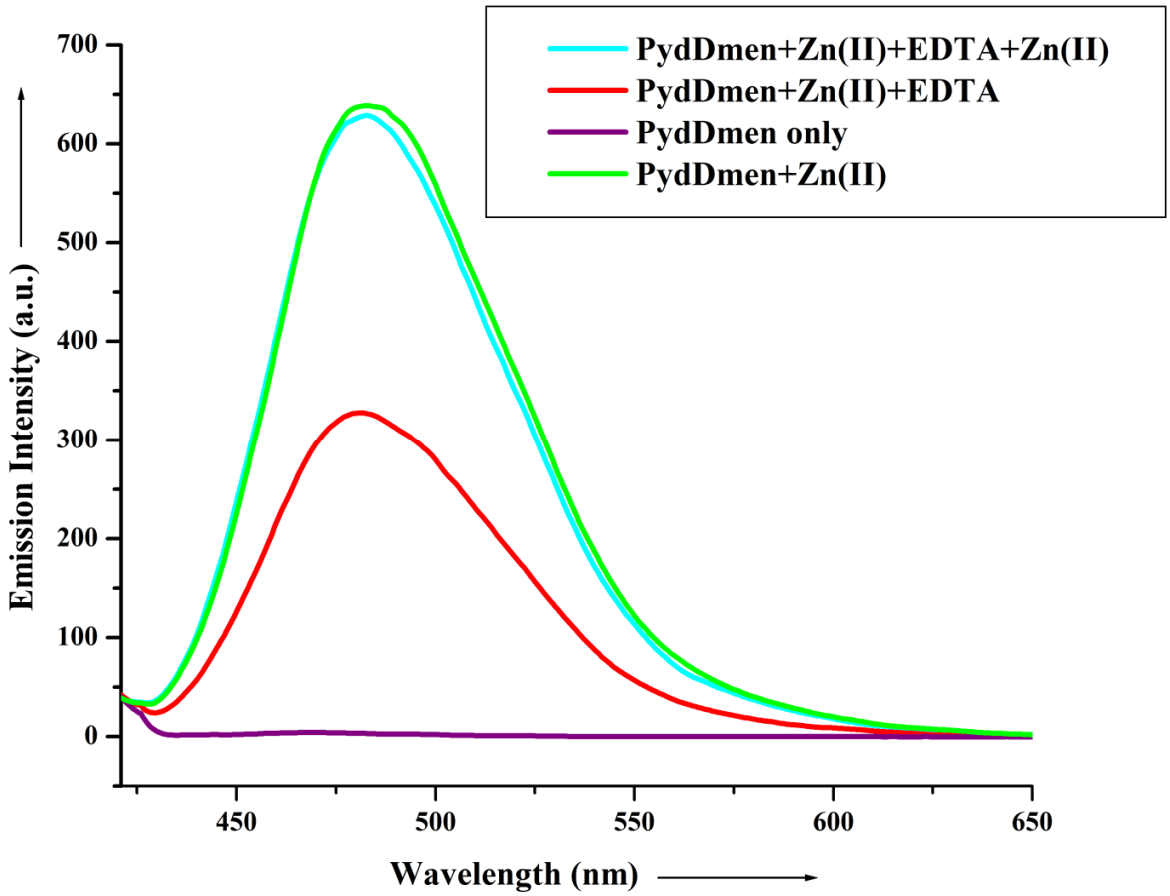

Figure S6: Fluorescence emission spectra of **PydDmen** in presence of Zn^{2+} ion followed by addition of Na_2EDTA (λ_{ex}=411 nm) and Zn^{2+} ion.

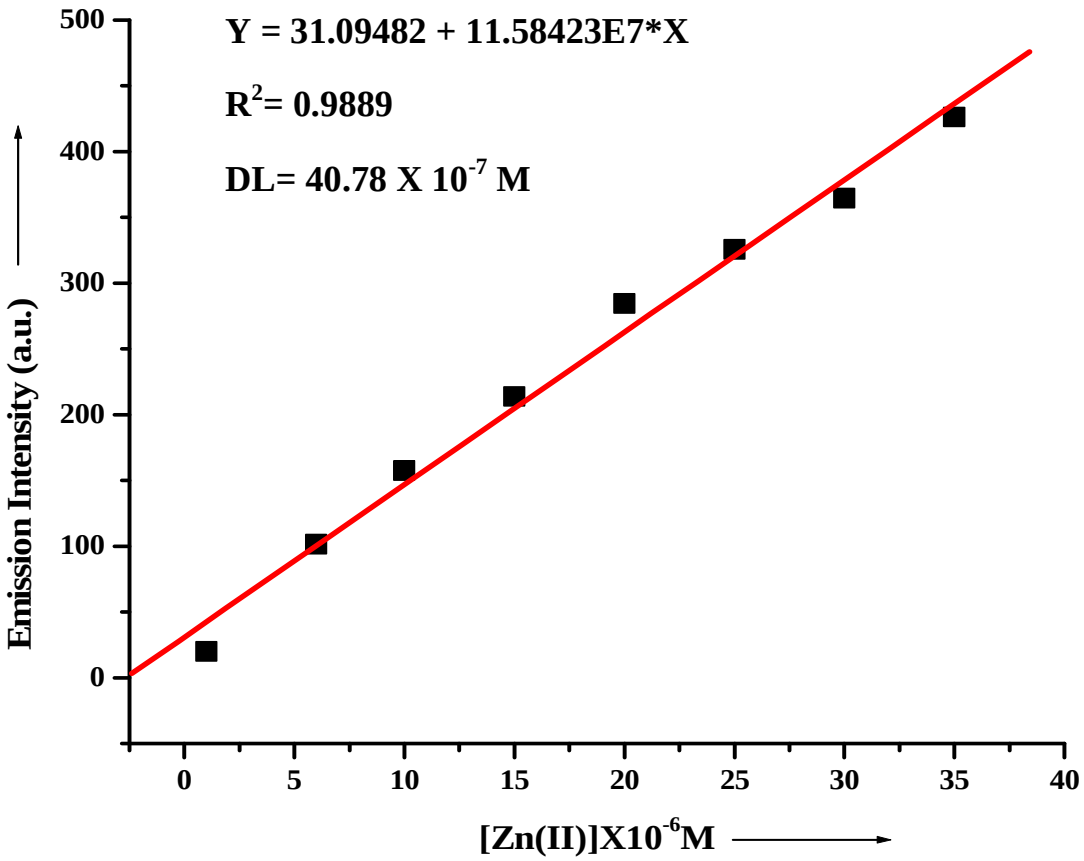

Figure S7: Determination of the detection limit of Zn^{2+} by **PydDmen** (5 x 10^{-6} M) in EtOH/ H_2O (4:1, v/v) in tris buffer at pH 7.4 (λ_{ex}=411 nm).

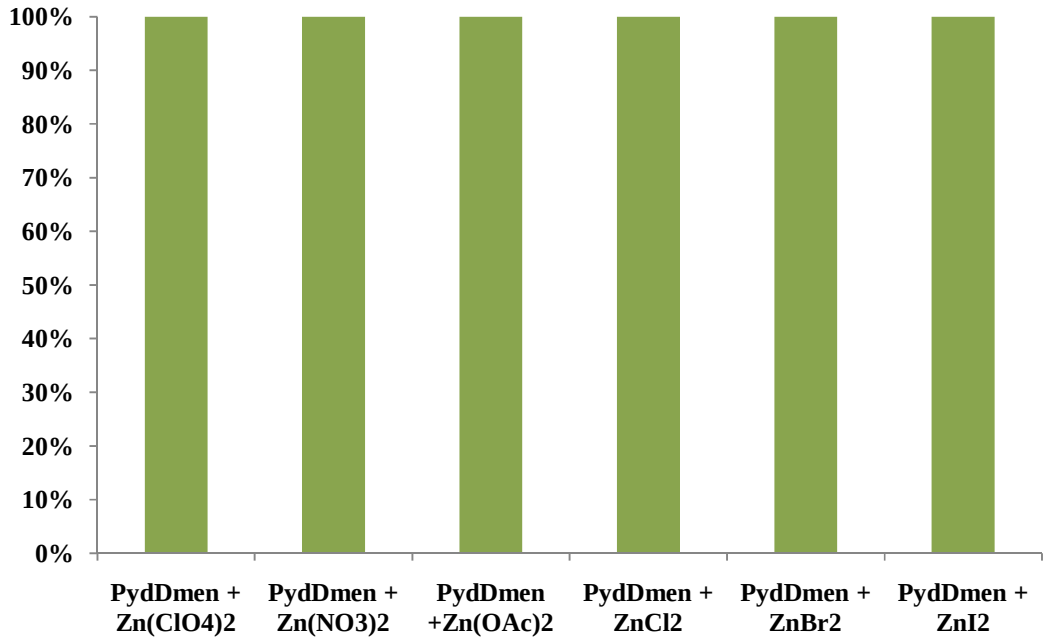

Figure S8: Relative emission intensity profile showing anion independency of **PydDmen** at 25°C in EtOH/ H_2O (4:1, v/v) in tris buffer at pH 7.4 (λ_{ex} =411 nm).

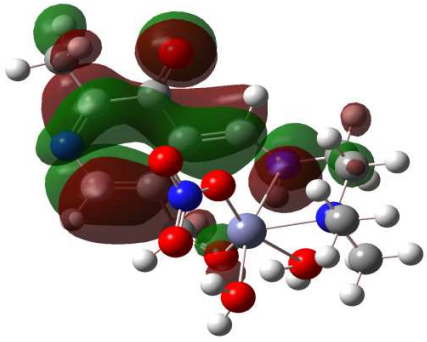

HOMO

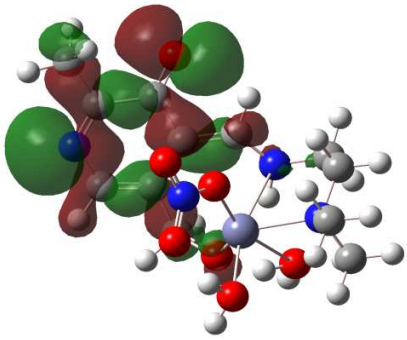

HOMO-1

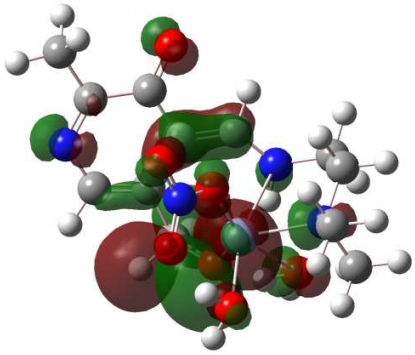

HOMO-2

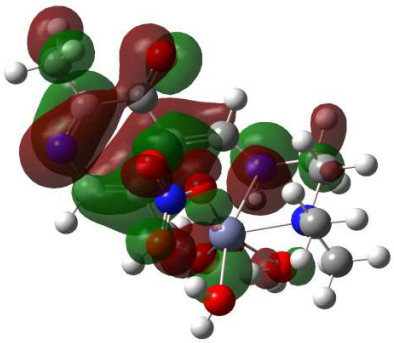

HOMO-3

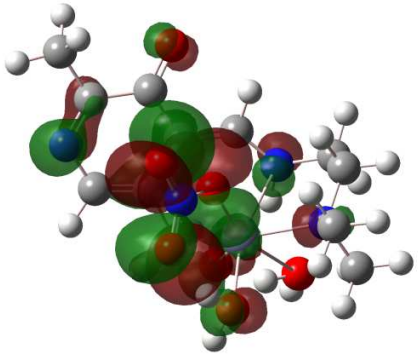

HOMO-4

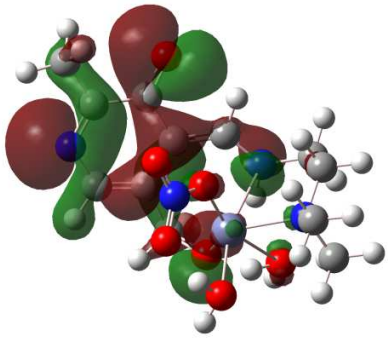

HOMO-5

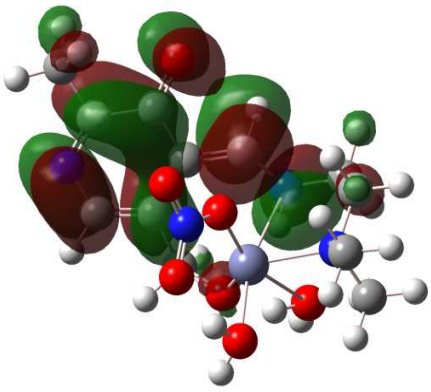

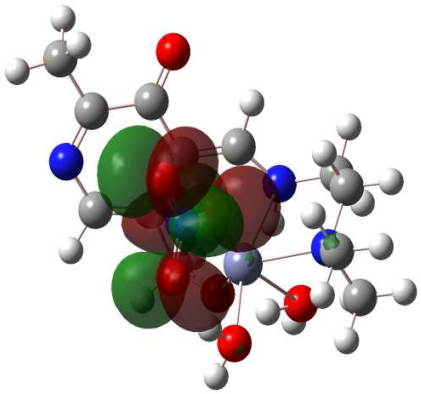

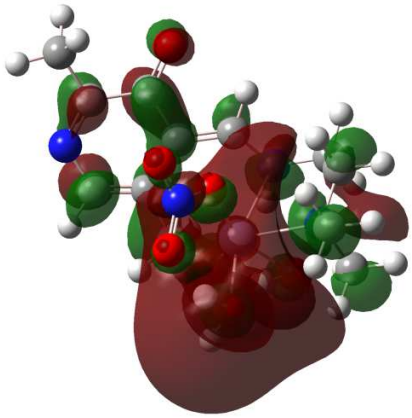

LUMO LUMO +1 LUMO +2

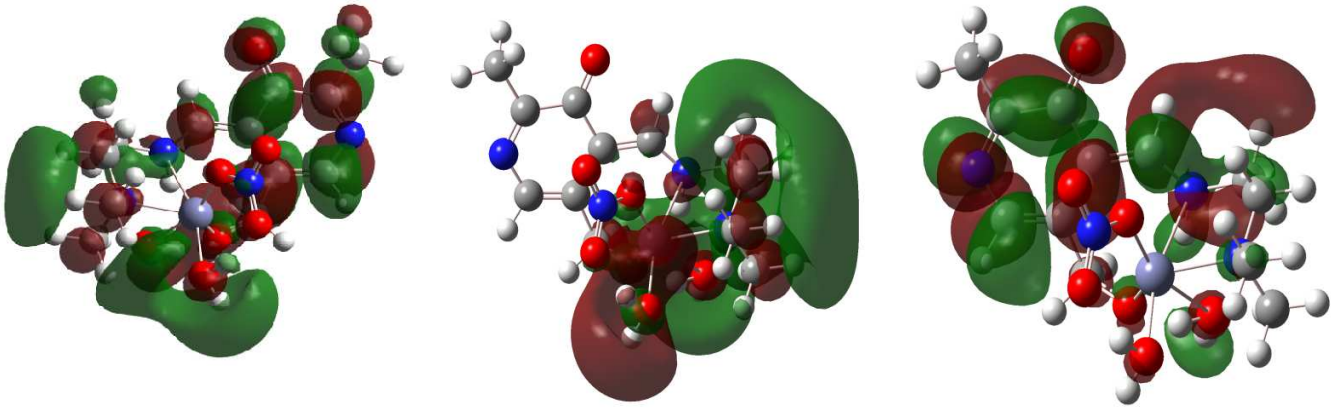

LUMO +3 LUMO +4 LUMO +5

Figure S9: Contour plots of some selected molecular orbitals of **PydDmen-Zn^{2+}.**

Table S1: Fluorescence lifetimes of chemosensor **PydDmen** and **PydDmen-Zn^{2+}** in EtOH/H_2O (4:1,v/v).

	τ_1(ns)	τ_2(ns)	τ_3(ns)	a_1	a_2	a_3	χ^2	τ_{av}	Φ	$k_r(s^{-1})\times10^9$	Fold w.r.t. **PydDmen**	k_{nr} $(s^{-1})\times 10^9$
PydDmen	0.821	3.375	9.334	0.349	0.243	0.406	1.089	3.79	0.094	0.0248	-	0.239
PydDmen -Zn^{2+}	1.479	9.078	-	0.112	0.888	-	1.1	8.23	0.408	0.0496	2	0.0719

Table S2: Changes in chemical shifts (δ ppm) of **PydDmen** during ^{1}H-NMR titration experiment upon gradual addition of $Zn(CH_3COO)_2.2H_2O$.

Equiv.	H_a	H_b	H_d	H_e	H_g	H_h
0.0	8.797	4.548	7.762	2.271	3.672	2.471
0.5	8.666	4.442	7.224	2.157	3.614	2.513
1.0	8.689	4.434	7.237	2.165	3.582	2.534
1.5	8.700	4.442	7.263	2.179	3.595	2.546
2.0	8.703	4.446	7.272	2.182	3.601	2.547

Table S3: Theoretical bond lengths and bond angles of **PydDmen-Zn^{2+}**.

Bonds (Å)	Calc.
Zn1-O2	1.87830
Zn1-O3	2.09134
Zn1-O4	3.66364
Zn1-O7	1.97689
Zn1-N2	2.84727
Zn1-N3	2.10894
Angles(°)	
O2-Zn1-O3	98.800
O2-Zn1-O4	108.829
O2-Zn1-O5	137.041
O2-Zn1-N2	71.650
O2-Zn1-N3	120.002
O3-Zn1-O4	108.829
O3-Zn1-O5	94.733
O3-Zn1-N2	159.937
O3-Zn1-N3	99.222
O4-Zn1-O5	156.413
O4-Zn1-N2	52.232
O4-Zn1-N3	78.168
O5-Zn1-N2	104.250
O5-Zn1-N3	97.462
N2-Zn1-N3	72.236

Table S4: Energy of selected MOs of **PydDmen-Zn^{2+}**.

MO	Energy (eV)
LUMO+5	0.64
LUMO+4	0.49
LUMO+3	0.39
LUMO+2	-0.28
LUMO+1	-1.19
LUMO	-2.26
HOMO	-5.54
HOMO-1	-5.95
HOMO-2	-7.16
HOMO-3	-7.30
HOMO-4	-7.41
HOMO-5	-7.55
HOMO-6	-7.82
HOMO-7	-8.43
HOMO-8	-8.63
HOMO-9	-8.69
HOMO-10	-8.79

Table S5: Vertical electronic transitions calculated by TDDFT/CPCM method for **PydDmen-Zn^{2+}** in ethanol.

$E_{excitation}$ (eV)	$\lambda_{excitation}$ (nm)	Osc. Strength (f)	Key transitions	Character
2.6848	461.81	0.0231	(69%) HOMO-1 → LUMO (31%) HOMO → LUMO	π(L) → π^*(L), ILCT π(L)→ π^*(L), ILCT
3.0345	408.58	0.2724	(31%) HOMO-1 → LUMO (69%) HOMO → LUMO	π(L) → π^*(L), ILCT π(L)/$p\pi$(o)→ π^*(L), ILCT
3.6541	339.30	0.0016	(71%) HOMO → LUMO+1	π(L) → π^*(L), ILCT
3.7591	329.83	0.0059	(70%) HOMO-2 → LUMO	π(L)/$p\pi$(o)→ π^*(L), ILCT
4.1860	296.19	0.0176	(23%) HOMO-6 → LUMO (26%) HOMO-4 → LUMO (51%) HOMO-3 → LUMO	π(L)/$p\pi$(o)→ π^*(L), ILCT π(L) → π^*(L), ILCT π(L) → π^*(L), ILCT
4.2580	291.18	0.0005	(16%)HOMO-5 → LUMO+1 (84%)HOMO-1 → LUMO+1	π(L) → π^*(L), ILCT π(L)/$p\pi$(o)→ π^*(L), ILCT
4.3687	283.80	0.0002	(12%)HOMO-7 → LUMO+1 (56%)HOMO-5→ LUMO+1 (10%)HOMO-4→ LUMO+1 (9%)HOMO-2→ LUMO+1 (12%)HOMO-1→ LUMO+1	π(L)/$p\pi$(o)→ π^*(L), ILCT π(L)/$p\pi$(o)→ π^*(L), ILCT π(L)/$p\pi$(o)→ π^*(L), ILCT π(L)/$p\pi$(o)→ π^*(L), ILCT π(L)/$p\pi$(o)→ π^*(L), ILCT

4.4266	280.09	0.0852	(36%) HOMO-6 → LUMO (31%) HOMO-4 → LUMO (32%) HOMO-3 → LUMO	π(L)/$p\pi$(o)→ π^*(L), ILCT π(L) → π^*(L), ILCT π(L) → π^*(L), ILCT
4.5150	274.61	0.0211	(47%) HOMO-6 → LUMO (52%) HOMO-4 → LUMO	π(L) → π^*(L), ILCT π(L)/$p\pi$(o)→ π^*(L), ILCT
4.5974	269.68	0.0057	(69%) HOMO-5 → LUMO	π(L)/$p\pi$(o)→ π^*(L), ILCT
4.8591	255.16	0.0006	(69%) HOMO-2→ LUMO +1	π(L)/$p\pi$(o)→ π^*(L), ILCT
5.1145	242.42	0.0057	(14%) HOMO-1→LUMO+2 (85%) HOMO→ LUMO+2	π(L)→ π^*(L), ILCT π(L)→ π^*(L), ILCT
5.1485	240.82	0.0009	(70%) HOMO-7→ LUMO	π(L)/$p\pi$(o)→ π^*(L), ILCT
5.2076	238.08	0.0013	(11%) HOMO-6 → LUMO (47%) HOMO-1 → LUMO+2 (18%) HOMO-1 → LUMO+3 (12%) HOMO-1 → LUMO+4 (10%) HOMO → LUMO+2	π(L)→ π^*(L), ILCT π(L)→ π^*(L), ILCT π(L)→ π^*(L), ILCT π(L)→ π^*(L), ILCT π(L)→ π^*(L), ILCT
5.2741	235.08	0.0009	(68%) HOMO-8→ LUMO	π(L)→ π^*(L), ILCT